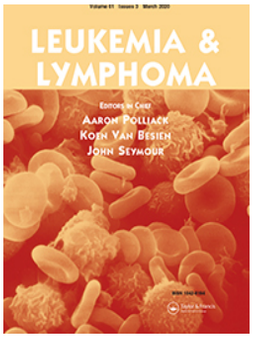

Leukemia & Lymphoma

ISSN: 1042-8194 (Print) 1029-2403 (Online) Journal homepage: https://www.tandfonline.com/loi/ilal20

STAT3, tumor microenvironment, and microvessel density in diffuse large B cell lymphomas

Roberto Tamma, Giuseppe Ingravallo, Francesco Gaudio, Tiziana Annese, Francesco Albano, Simona Ruggieri, Michele Dicataldo, Eugenio Maiorano, Giorgina Specchia & Domenico Ribatti

To cite this article: Roberto Tamma, Giuseppe Ingravallo, Francesco Gaudio, Tiziana Annese, Francesco Albano, Simona Ruggieri, Michele Dicataldo, Eugenio Maiorano, Giorgina Specchia & Domenico Ribatti (2020) STAT3, tumor microenvironment, and microvessel density in diffuse large B cell lymphomas, Leukemia & Lymphoma, 61:3, 567-574, DOI: 10.1080/10428194.2019.1678154

To link to this article: https://doi.org/10.1080/10428194.2019.1678154

Published online: 17 Oct 2019.

LEUKEMIA & LYMPHOMA
2020, VOL. 61, NO. 3, 567–574
https://doi.org/10.1080/10428194.2019.1678154

Taylor & Francis
Taylor & Francis Group

ORIGINAL ARTICLE

STAT3, tumor microenvironment, and microvessel density in diffuse large B cell lymphomas

Roberto Tamma[a], Giuseppe Ingravallo[b], Francesco Gaudio[c], Tiziana Annese[a], Francesco Albano[c], Simona Ruggieri[a], Michele Dicataldo[b], Eugenio Maiorano[b], Giorgina Specchia[c] and Domenico Ribatti[a]

[a]Department of Basic Medical Sciences, Neurosciences, and Sensory Organs, University of Bari Medical School, Bari, Italy; [b]Department of Emergency and Transplantation, Pathology Section, University of Bari Medical School, Bari, Italy; [c]Department of Emergency and Transplantation, Hematology Section, University of Bari Medical School, Italy

ABSTRACT

Constitutively activated STAT3 is correlated with more advanced clinical stage and overall poor survival of diffuse large B-cell lymphoma (DLBCL). The aim of this study was to evaluate STAT3 and Ki67 tumor cell expression, inflammatory cell infiltration, microvascular density in DLBCL bioptic specimens. RNA-scope showed that activated B cell (ABC) tissue samples contained a significant higher number of STAT3+ cells as compared to germinal center B (GCB) tissue samples. Immunohistochemical analysis showed a significant increased levels of CD3, CD8, CD68, CD163, CD34, and Ki67 positive cells in ABC patients. A positive correlation between STAT3 and CD3, CD8, CD68, and CD163 was evidenced in ABC group. In ABC group, we found also a positive correlation between CD8 and CD34 and a positive correlation between Ki67 and, CD68, and CD163. These data indicate that in ABC—as compared to GCB-DLBCL, a higher STAT3 expression is associated with a higher CD163+ TAM and CD8+ cell infiltration which induces a strong angiogenic response.

ARTICLE HISTORY
Received 16 August 2019
Revised 21 September 2019
Accepted 30 September 2019

KEYWORDS
DLBCL lymphomas; lymphocytes; RNAscope; STAT3; tumor-associated macrophages

Introduction

Diffuse large B-cell lymphoma (DLBCL) is one of the most frequent types of lymphoid neoplasia and accounts for 30–40% of cases of non-Hodgkin's lymphomas (NHL) [1]. DLBCLs is highly heterogeneous at both clinical and biological levels arising from germinal center B-cells at different stages of differentiation, in which recurrent genetic alterations contribute to the molecular pathogenesis of the disease [2,3].

The definition of aggressive lymphoma reflects a clinical concept associated with different histological subtypes, characterized by a rapid clinical course and a brief survival in cases not adequately treated or not responsive to treatment [4]. The incidence of aggressive forms is partly associated to its increase in patients with AIDS or subjected to immunosuppressive therapy after organ or bone marrow transplantation [5].

Gene expression profiling technique allowed to identify at least two molecular subtypes of DLBCL with different prognoses [6]. The first one is the lymphoma derived from the germinal center B (GCB) and the second one is the lymphoma derived from the activated B cell (ABC). Specific markers, including CD10, LMO2, and BCL6, are expressed in GCB patients, which respond better to conventional chemotherapy, whereas ABC patients express lower levels of BCL6 and are refractory to chemotherapy [6,7].

Improvement in the knowledge of the hematological malignancies pathogenesis derives from the study of the inflammatory cells in the tumor microenvironment [8] and of the genetic and epigenetic changes in malignant cells strictly related to the generation of an inflammatory microenvironment that further supports tumor progression [9].

Experimental evidences suggest a crucial role for signal transducer and activator of transcription-3 (STAT3) in selectively induce and maintain a pro-carcinogenic inflammatory microenvironment [10–12].

Constitutively activated STAT3 is correlated with more advanced clinical stage and overall poor survival of DLBCL and its activation represents an oncogenic pathway in ABC-DLBCL providing an additional therapeutic target [13–15]. Moreover, in ABC-DLBCL the activation of Janus kinases (JAKs)/STAT3 pathway correlates with autocrine production of interleukins 6 and

CONTACT Domenico Ribatti domenico.ribatti@uniba.it Department of Basic Medical Sciences, Neurosciences and Sensory Organs, University of Bari Medical School, Policlinico - Piazza G. Cesare, 11, 70124 Bari, Italy

10 (IL-6 and IL-10), which promotes cancer progression [12,16].

We have previously demonstrated a greater expression of STAT3 in ABC-DLBCL patients as compared to the GCB ones and its implication in tumor vessel constitution [15], and significant increase in the expression of CD68+ tumor-associated macrophages (TAMs) as well as a significant increase in microvascular density in a group of chemo-resistant DLBCL patients as compared to a group of chemo-sensitive ones [17].

In this study, we have correlated the expression of STAT3 by RNA-scope assay in ABC and GCB groups with the tumor cells Ki67 proliferation index and the characteristics of the tumor inflammatory microenvironment by the evaluation of CD68+ and CD163+ macrophages, CD3+ and CD8+ lymphocytes, and CD34+ vessels by immunohistochemistry and morphometric estimation.

Materials and methods

Patients

This retrospective study reviewed data from 60 patients diagnosed with DLBCL collected from the archive of the Section of Pathology of Department of Emergency and Transplantation, University of Bari Medical School, Bari, Italy, between 2009 and 2017. All procedures were in accordance with the ethical standards of the responsible committee on human experimentation (institutional and national) and with the Helsinki Declaration of 1964 and later versions, and signed informed consent from individual patients were obtained to conduct the study. All patients had pathologically confirmed DLBCL. Tumors were divided into two histological subgroups: one that includes 30 ABC patients and another that includes 30 GCB patients.

STAT3 RNAscope assay

RNAscope assay was performed on FFPE biopsies using RNAscope 2.5 HD Reagent Kit [RED 322360, Advanced Cell Diagnostics (ACD), Hayward, CA]. Briefly, tissue sections were deparaffinized with xylene and 100% ethanol and incubated with pretreat-1 solution for 10 min, pretreat-2 for 15 min, and pretreat-3 for 30 min (Pretreatment kit 322330, ACD). The slides were then hybridized with a probe Hs-STAT3 (ref. 425631), positive control probe—Hs-PPIB (ref. 313901), negative control probe—DapB (ref. 310043) in the HybEZ oven (ACD) at 40 °C for 2 h. The Hs-PPIB probe for human housekeeping gene PPIB was used as a control to ensure RNA quality. After hybridizations, slides were subjected to signal amplification using HD 2.5 detection Kit, and hybridization signal was detected using a mixture of Fast-RED solutions A and B (1:60). After counterstaining with Gill's hematoxylin, slides were dried in a 60 °C dry oven for 15 min and mounted with Glycergel Mounting Medium (Dako, C0563). Sections from each experimental group were scanned using the whole-slide morphometric analysis scanning platform Aperio Scanscope CS (Leica Biosystems, Nussloch, Germany). All the slides were scanned at the maximum available magnification (40×) and stored as digital high-resolution images on the workstation associated with the instrument. Based on the PPIB evaluation, all the cases were included in the analysis. Digital slides were inspected with Aperio ImageScope v.11 software (Leica Biosystems, Nussloch, Germany) at 20× magnification and 10 fields with an equal area were selected for the analysis at 40× magnification. The mRNA expression was assessed by Aperio RNA ISH algorithm that provides standardized quantitation of RNA ISH staining in whole slide images of FFPE tissue. This algorithm automatically quantifies the staining across whole slides, counts individual molecular signals and clusters in the cells. The obtained results are divided in three ranges: 1+ that includes cells containing 2–5 dots for cell; 2+ that include cells containing 6–20 dots for cell; 3+ that include cells containing more than 20 dots for cell. The statistical significance of differences between the mean values of the percent labeled areas between ABC and GCB tumor specimens were determined by the two-way ANOVA test in GraphPad Prism 5.0 software (GraphPad Software, La Jolla, CA). Findings were considered significant at p values $<.05$.

CD3, CD8, CD68, CD163, CD34, and Ki67 immunohistochemistry

Histological sections of 4 μm thickness, collected on poly-L-lysine-coated slides (Sigma Chemical, St Louis, MO), were deparaffinized. The sections were rehydrated in a xylene-graded alcohol scale and then rinsed for 10 min in 0.1 M PBS. Sections were pretreated with sodium citrate pH 6.1 solution (DAKO, Glostrup, Denmark) for antigen retrieval for 30 min at 98 °C and then incubated with mouse monoclonal anti-CD3 (DAKO, Glostrup, Denmark), mouse monoclonal anti-CD8 (DAKO, Glostrup, Denmark), mouse monoclonal anti-CD68 (DAKO, Glostrup, Denmark), mouse monoclonal anti-CD163 (DAKO, Glostrup, Denmark), mouse monoclonal anti-CD34 (DAKO,

Glostrup, Denmark) and mouse monoclonal anti-ki67 (DAKO, Glostrup, Denmark) diluted 1:100, 1:50, 1:100, 1:100, 1:100, and 1:25, respectively. Thereafter, the sections were counterstained with Mayer hematoxylin and mounted in synthetic medium. Specific preimmune serum (Dako), replacing the primary antibodies, served as negative control. Sections from each experimental group (n.10), 30 cases per group, were scanned using the whole-slide morphometric analysis scanning platform Aperio Scanscope CS (Leica Biosystems, Nussloch, Germany). All the slides were scanned at the maximum available magnification (40×) and stored as digital high-resolution images on the workstation associated with the instrument. Digital slides were inspected with Aperio ImageScope v.11 software (Leica Biosystems, Nussloch, Germany) at 20× magnification and 10 fields with an equal area were selected for the analysis at 40× magnification. The protein expression was assessed with the Positive Pixel Count algorithm embedded in the Aperio ImageScope software and reported as positivity percentage, defined as the number of positively stained pixels on the total pixels in the image. The statistical significance of differences between the mean values of the percent labeled areas between tumor breast specimens and control tissues was determined by the two-way Anova test in GraphPad Prism 5.0 software (GraphPad software, La Jolla, CA). Findings were considered significant at $p < .05$.

Statistical analysis

Data related to the two experimental groups: ABC- and GCB-DLBCL patients, are reported as means ± SEM. Newman–Keuls multiple comparisons post-test was used to compare all treatment groups after one-way ANOVA. The Graph Pad Prism 5.0 statistical package (GraphPad Software, San Diego, CA) was used for analyses and the limit for statistical significance was set at $p < .05$. Correlation analysis was performed with the Spearman non parametric correlation test. The Graph Pad Prism 5.0 statistical package (GraphPad Software, San Diego, CA) was used for analyses and the limit for statistical significance was set at $p < .05$.

Results

RNAscope-STAT3 expression

RNAscope assay was performed in order to evaluate the expression of STAT3 mRNA in tumor cells in both ABC and GCB groups of DLBCL tissue samples (Figure 1). Three groups of data have been considered according

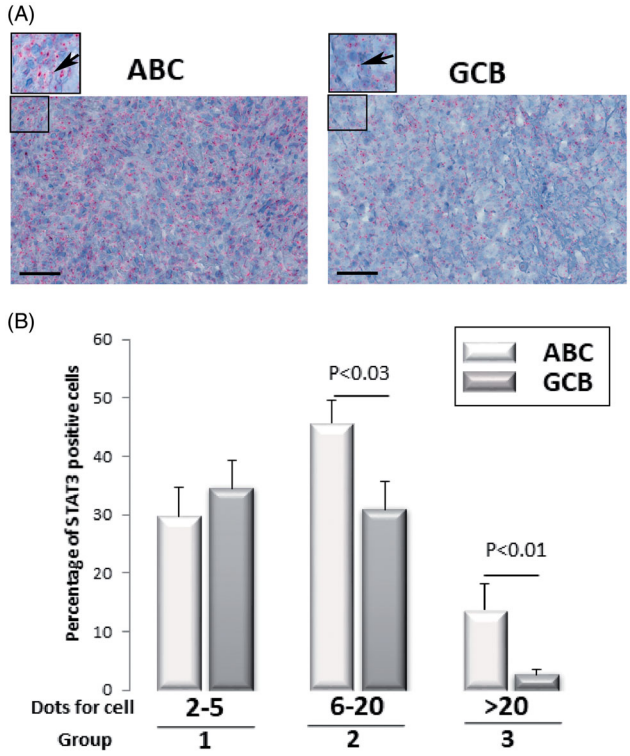

Figure 1. (A) RNAscope-STAT3 mRNA expression in histological samples of ABC- and GCB-DLBCL groups. Arrows indicate the dots in the higher magnification insert. Scale bar: 60 μm. (B) Quantitation of RNA ISH staining of STAT3 mRNA positivity in ABC- and GCB-DLBCL samples. The per cent of STAT3 mRNA expressing cells significantly increases in the ABC groups 2 and 3 tumor samples compared to GCB.

to the number of STAT3 positive signals (red dots) (Figure 1(A)) contained in each cell. Group 1 included the percentage of cells containing from 2 to 5 dots, group 2 included the percentage of cells containing from 6 to 20 dots, and group three included the percentage of cells containing more than 20 dots. ABC tissue samples contained a significant higher number of positive cells in both group 2 and 3, as compared to GCB tissue samples. It was not evidenced significant differences between cells belonging to the group 1 in ABC and GCB experimental groups. Figure 1(B) shows morphometric analysis of the STAT3 expression in ABC/Group 1 (29.6% ± SE 4.9%), ABC/Group 2 (45.7% ± SE 3.9%), and ABC/Group 3 (13.7% ± SE 4.3%), as compared to GCB/group 1 (34.6% ± SE 4.7%), GCB/Group 2 (30.9% ± SE 4.7%), and GBC/Group 3 (2.6% ± SE 0.7%).

CD3, CD8, CD68, CD163, CD34, and Ki67 immunohistochemistry

ABC and GCB DLBCL specimens were immunostained for CD3, CD8, CD68, CD163, CD34, and Ki67 in order

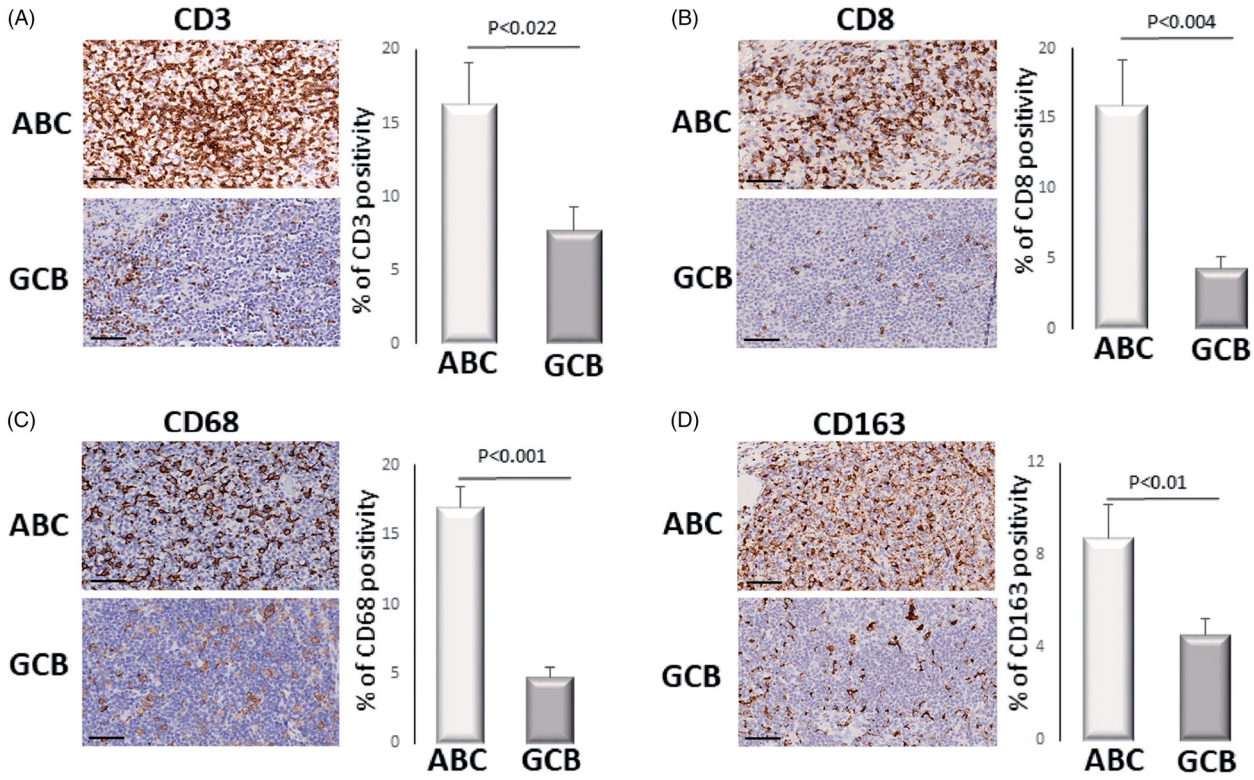

Figure 2. Immunohistochemical staining of CD3 (A), CD8 (B), CD68 (C), CD163 (D) in ABC- and GCB-DLBCL samples. Scale bar: A-D 60 μm. Morphometric analysis expressed in per cent of CD3 (A), CD8 (B), CD68 (C), CD163 (D) in ABC- and GCB-DLBCL samples.

to estimate CD3+ lymphocytes (Figure 2(A)), $CD8^+$ lymphocytes (Figure 2(B)), CD68+ macrophages (Figure 2(C)), CD163+ macrophages (Figure 2(D)), CD34+ microvessels (Figure 3(A)), and Ki67+ cells (Figure 3(B)). Morphometric analysis (Figures 2 and 3) shows the significant increased levels of CD3, CD8, CD68, CD163, CD34, and Ki67 cells in ABC group (CD3: 16.3% ± SE 2.8%; CD8: 15.9 % ±SE 3.3%; CD68: 17% ± SE 1.15%; CD163: 8.73% ± SE 1.5%; CD34: 4% ± SE 0.6%; Ki 16% ± SE 1.5%) as compared to the GCB group (CD3: 7.6% ± SE 1.65%; CD8: 4.3% ± SE 0,86%; CD68: 4.8%±SE 1.4%; CD163: 4,6% ± SE 0.7%; CD34: 1.6% ± SE 0.13%; Ki67 11% ± SE 0.7%).

A correlation study on the relationship between STAT3 expression and the other evaluated markers was also performed in both ABC and GCB group (Figure 4(A)). A positive correlation between STAT3 and CD3 (rho = 0.6, $p = .04$), CD8 (rho = 0.8, $p = .002$), CD68 (rho = 0.7, $p = .01$), CD163 (rho = 0.8, $p = .001$) in ABC DLBCL samples was found as assessed by Spearman correlation analysis. In DLBCL ABC group we found a positive correlation between CD8 and CD34 (rho = 0.7, $p = .0005$) (Figure 4(B)). Moreover, we also found a positive correlation between Ki67 and, CD68 (rho = 0.8, $p = .001$), CD163 (rho = 0.6, $p = .002$) in ABC DLBCL samples (Figure 4(C)).

Discussion

STAT3 factor is activated by numerous cytokines, growth factors, and oncogenes, and is constitutively active in hematological as well as solid tumors [12,18–22]. STAT3 and the genes that it regulates are involved in promoting tumor cell proliferation, survival [23], angiogenesis, and metastasis [11,24–26], and interfere with apoptosis and anti-tumor immune responses [27,28]. STAT3 is also studied as a target for anti-cancer therapy [29–31].

Constitutive phosphorylation and activation of STATs have been found in acute myeloid leukemia, acute promyelocytic leukemia, acute lymphoblastic leukemia (ALL), chronic lymphocytic leukemia (CLL), and chronic myelogenous leukemia (CML) [32–34]. In leukemia patients and in particular in large granular lymphocytic leukemia, mutations in the SH2 domain of STAT3 have been observed indicating its relation in the pathogenesis of these diseases [35,36].

Multiple myeloma (MM) has been reported the involvement of some major signaling pathways including the JAK-STAT3, PI3K/Akt/mTOR, and NF-κB [37,38]. It is believed that STAT3 might be constitutively active or activated by the interleukin-6(IL-6)-JAK-STAT3 axis [39]. STAT3 activation is associated with poor prognosis and

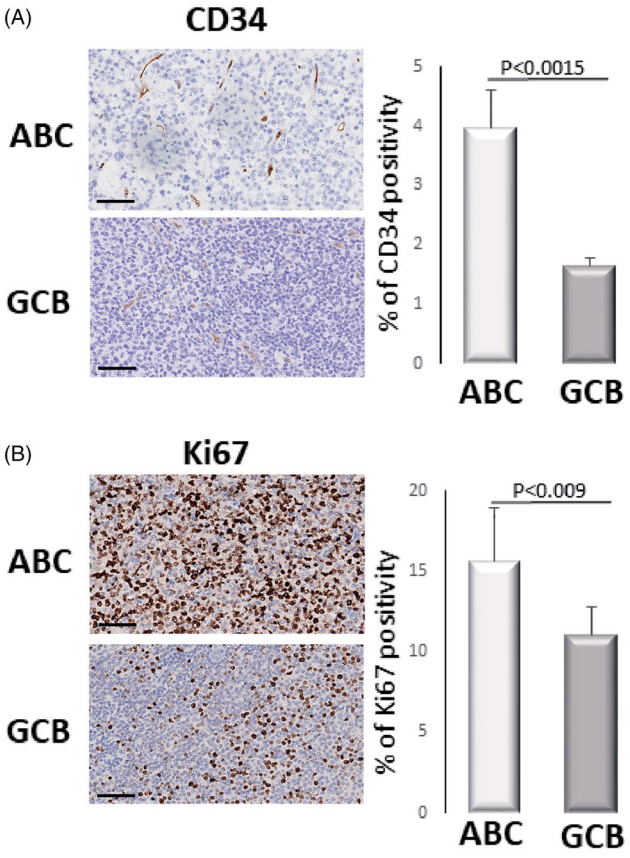

Figure 3. Immunohistochemical staining of CD34 (A) and Ki67 (B) in ABC- and GCB-DLBCL samples. Scale bar: A–D 60 μm. Morphometric analysis expressed in per cent of CD34 (A) and Ki67 (B) in ABC- and GCB-DLBCL samples.

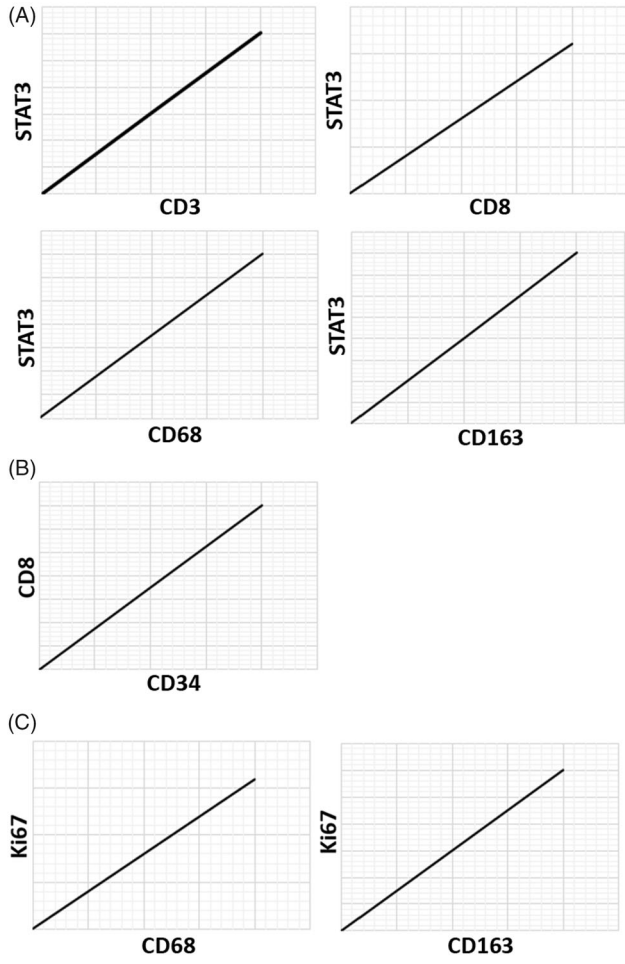

Figure 4. Regression graph between: (A) STAT3 and CD3, CD8, CD68, CD163; (B) CD8 and CD34; (C) Ki67 and CD68, CD163; in ABC- and GCB-DLBCL samples.

survival in MM patients. Inhibition of STAT3 signaling inhibits tumor growth, re-sensitizes to therapy, and induces apoptosis [40–42].

In several Hodgkin lymphoma cell lines, as well as primary Hodgkin's Reed–Sternberg cells constitutive phosphorylation of STAT1 and STAT3 it is thought to lead to inappropriate expression of downstream genes including *Bcl-2* and *Bcl-xL* that have been involved in cell survival and apoptosis regulation [43,44]. JNK and JAK/STAT pathways could stimulate cell proliferation and xenograft growth in various NHL cell lines. This effect is due to the formation of a transcriptional between p-STAT3/p-c-Jun/ISL-1 (Insulin Enhancer Binding Protein 1) [45]. Targeted oligonucleotides against STAT3 in nude mice exert a therapeutic effect against human DLBCL xenotransplants by a direct cytotoxic/cytostatic effect [46]. In primary cutaneous T-cell lymphomas (CTCL) and anaplastic large T-cell lymphoma (ALCL), it has been demonstrated an aberrant expression of both STAT3 and STAT5, and the inhibition of these two proteins inhibits tumor growth [47].

An elevated expression of STAT3 is associated with poor prognosis in DLBCL [12,14]. We have previously demonstrated that STAT3 expression, estimated by using RNA-scope assay, a new and highly sensitive method for oligonucleotide detection, is higher in ABC-DLBCL as compared with GBC-DLBCL [15].

The results of this study have confirmed a higher expression of STAT3 in ABC group. Moreover, we have also demonstrated a higher Ki67 expression in tumor cells and a higher number of CD163+ macrophages in ABC patients as compared with GBC ones.

In tumors, inflammation precede development of malignancy, and tumor-infiltrated inflammatory cells act in concert with tumor cells, stromal cells and endothelial cells to create a microenvironment that is critical for the survival, development and dissemination of the neoplastic mass [48,49]. These interactions within the tumor microenvironment may represent important mechanisms for tumor development and metastasis by providing an efficient vascular supply and an easy escape pathway.

Among inflammatory cells that have been identified as modifiers of tumor microenvironment, mast cells, macrophages, and lymphocytes play a crucial role. Cells infiltrating the tumor microenvironment and all their secreted factors including cytokines, growth factors, and chemokines influence positively or negatively the tumorigenic process through the balance of pro- and anti-inflammatory factors, their relative concentrations, their receptor expression content, and the activation state of surrounding cells [49].

TAMs are divided in two major subsets: the M1 involved in antitumor immunity and anti-angiogenesis and the M2 ones which have the opposing roles of enhancing immunosuppression and angiogenesis [50]. Experimental evidences suggest that TAMs, are likely involved in tumor progression via STAT3 activation [51–56]. The M2 phenotype is involved in tumor initiation and progression [57]. Moreover, it has been suggested a possible correlation between a high M2 number and an unfavorable prognosis in patients with DLBCL [56,58].

In this study, we have also demonstrated a significant higher number of CD3+ and CD8+ cells ABC group as compared with GBC one. Moreover, CD8+ cell number correlates with STAT3 expression and microvascular density in ABC patients. In DLBCL tumor microenvironment a low T-cell infiltration seems to correlate with poor survival, even if the prognostic value of CD4/CD8 ratio has been associated with both better and worse survival in different studies [59,60]. We found no variation in CD4+ cells in ABC respect to GCB (data not shown) but a higher CD8+ cell infiltrate in ABC group associated with a decreased CD4/CD8 ratio. The correlation between CD8+ lymphocytes and CD34+ microvessels in ABC patients observed in this study indicates that CD8+ lymphocytes promote angiogenesis in DLBCL.

Overall, these data indicate that in ABC-DLBCL as compared with GCB-DLBCL, a higher STAT3 expression is associated with a higher M2 TAM and CD8+ cell infiltration the tumor microenvironment which, in turn, induces a strong angiogenic response in ABC group.

Disclosure statement

No potential conflict of interest was reported by the authors.

Funding

This work has been supported by the Associazione “Il Sorriso di Antonio”, Corato, Italy.

ORCID

Francesco Albano http://orcid.org/0000-0001-7926-6052
Michele Dicataldo http://orcid.org/0000-0003-0385-9040
Domenico Ribatti http://orcid.org/0000-0003-4768-8431

References

[1] Campo E, Swerdlow SH, Harris NL, et al. The 2008 WHO classification of lymphoid neoplasms and beyond: evolving concepts and practical applications. Blood. 2011;117(19):5019–5032.
[2] Schneider C, Pasqualucci L, Dalla-Favera R. Molecular pathogenesis of diffuse large B-cell lymphoma. Semin Diagn Pathol. 2011;28(2):167–177.
[3] Miao Y, Medeiros LJ, Li Y, et al. Genetic alterations and their clinical implications in DLBCL. Nat Rev Clin Oncol. 2019;16(10):634.
[4] Armitage JO, Gascoyne RD, Lunning MA, et al. Non-Hodgkin lymphoma. Lancet. 2017;390(10091):298–310.
[5] Barta SK, Samuel MS, Xue X, et al. Changes in the influence of lymphoma- and HIV-specific factors on outcomes in AIDS-related non-Hodgkin lymphoma. Ann Oncol. 2015;26(5):958–966.
[6] Alizadeh AA, Eisen MB, Davis RE, et al. Distinct types of diffuse large B-cell lymphoma identified by gene expression profiling. Nature. 2000;403(6769):503–511.
[7] Rosenwald A, Wright G, Chan WC, et al. The use of molecular profiling to predict survival after chemotherapy for diffuse large-B-cell lymphoma. N Engl J Med. 2002;346(25):1937–1947.
[8] Mulder TA, Wahlin BE, Osterborg A, et al. Targeting the immune microenvironment in lymphomas of B-cell origin: from biology to clinical application. Cancers (Basel). 2019;11:pii: E915.
[9] Mantovani A, Allavena P, Sica A, et al. Cancer-related inflammation. Nature. 2008;454(7203):436–444.
[10] Catlett-Falcone R, Landowski TH, Oshiro MM, et al. Constitutive activation of Stat3 signaling confers resistance to apoptosis in human U266 myeloma cells. Immunity. 1999;10(1):105–115.
[11] Kujawski M, Kortylewski M, Lee H, et al. Stat3 mediates myeloid cell-dependent tumor angiogenesis in mice. J Clin Invest. 2008;118(10):3367–3377.
[12] Ding BB, Yu JJ, Yu RY, et al. Constitutively activated STAT3 promotes cell proliferation and survival in the activated B-cell subtype of diffuse large B-cell lymphomas. Blood. 2007;111(3):1515–1523.
[13] Ok CY, Chen J, Xu-Monette ZY, et al. Clinical implications of phosphorylated STAT3 expression in De Novo diffuse large B-cell lymphoma. Clin Cancer Res. 2014;20(19):5113–5123.
[14] Wu ZL, Song YQ, Shi YF, et al. High nuclear expression of STAT3 is associated with unfavorable prognosis in diffuse large B-cell lymphoma. J Hematol Oncol. 2011;4:31.
[15] Tamma R, Ingravallo G, Albano F, et al. STAT-3 RNAscope determination in human diffuse large B-cell lymphoma. Transl Oncol. 2019;12(3):545–549.
[16] Lam LT, Wright G, Davis RE, et al. Cooperative signaling through the signal transducer and activator of transcription 3 and nuclear factor-{kappa}B pathways

in subtypes of diffuse large B-cell lymphoma. Blood. 2008;111(7):3701–3713.
[17] Marinaccio C, Ingravallo G, Gaudio F, et al. Microvascular density, CD68 and tryptase expression in human diffuse large B-cell lymphoma. Leuk Res. 2014;38(11):1374–1377.
[18] Yu H, Lee H, Herrmann A, et al. Revisiting STAT3 signalling in cancer: new and unexpected biological functions. Nat Rev Cancer. 2014;14(11):736–746.
[19] Avalle L, Camporeale A, Camperi A, et al. STAT3 in cancer: a double edged sword. Cytokine. 2017;98: 42–50.
[20] Ruggieri S, Tamma R, Resta N, et al. Stat3-positive tumor cells contribute to vessels neoformation in primary central nervous system lymphoma. Oncotarget. 2017;8(19):31254–31269.
[21] Yuan J, Zhang F, Niu R. Multiple regulation pathways and pivotal biological functions of STAT3 in cancer. Sci Rep. 2016;5(1):17663.
[22] Alas S, Bonavida B. Inhibition of constitutive STAT3 activity sensitizes resistant non-Hodgkin's lymphoma and multiple myeloma to chemotherapeutic drug-mediated apoptosis. Clin Cancer Res. 2003;9(1): 316–326.
[23] Lin L, Liu A, Peng Z, et al. STAT3 is necessary for proliferation and survival in colon cancer-initiating cells. Cancer Res. 2011;71(23):7226–7237.
[24] Chang Q, Bournazou E, Sansone P, et al. The IL-6/JAK/Stat3 feed-forward loop drives tumorigenesis and metastasis. Neoplasia. 2013;15(7):848–862.
[25] Kamran MZ, Patil P, Gude RP. Role of STAT3 in cancer metastasis and translational advances. Biomed Res Int. 2013;2013:1.
[26] Matsukawa A, Kudo S, Maeda T, et al. Stat3 in resident macrophages as a repressor protein of inflammatory response. J Immunol. 2005;175(5):3354–3359.
[27] Johnston PA, Grandis JR. STAT3 signaling: anticancer strategies and challenges. Mol Interv. 2011;11(1): 18–26.
[28] Gritsina G, Xiao F, O'Brien SW, et al. Targeted blockade of JAK/STAT3 signaling inhibits ovarian carcinoma growth. Mol Cancer Ther. 2015;14(4):1035–1047.
[29] Sgrignani J, Garofalo M, Matkovic M, et al. Structural biology of STAT3 and its implications for anticancer therapies development. Int J Mol Sci. 2018;19:pii: E1591.
[30] Siveen KS, Sikka S, Surana R, et al. Targeting the STAT3 signaling pathway in cancer: role of synthetic and natural inhibitors. Biochim Biophys Acta. 2014; 1845:136–154.
[31] Lu L, Zhu F, Zhang M, et al. Gene regulation and suppression of type I interferon signaling by STAT3 in diffuse large B cell lymphoma. Proc Natl Acad Sci USA. 2018;115(3):E498–E505.
[32] Gouilleux-Gruart V, Gouilleux F, Desaint C, et al. STAT-related transcription factors are constitutively activated in peripheral blood cells from acute leukemia patients. Blood. 1996;87(5):1692–1697.
[33] Frank DA, Mahajan S, Ritz J. B lymphocytes from patients with chronic lymphocytic leukemia contain signal transducer and activator of transcription (STAT) 1 and STAT3 constitutively phosphorylated on serine residues. J Clin Invest. 1997;100(12):3140–3148.
[34] Munoz J, Dhillon N, Janku F, et al. STAT3 inhibitors: finding a home in lymphoma and leukemia. Oncologist. 2014;19(5):536–544.
[35] Koskela HL, Eldfors S, Ellonen P, et al. Somatic STAT3 mutations in large granular lymphocytic leukemia. N Engl J Med. 2012;366(20):1905–1913.
[36] Shahmarvand N, Nagy A, Shahryari J, et al. Mutations in the signal transducer and activator of transcription family of genes in cancer. Cancer Sci. 2018;109(4): 926–933.
[37] Hu J, Hu WX. Targeting signaling pathways in multiple myeloma: Pathogenesis and implication for treatments. Cancer Lett. 2018;414:214–221.
[38] Podar K, Chauhan D, Anderson KC. Bone marrow microenvironment and the identification of new targets for myeloma therapy. Leukemia. 2009;23(1): 10–24.
[39] Ramakrishnan V, Kimlinger T, Haug J, et al. TG101209, a novel JAK2 inhibitor, has significant in vitro activity in multiple myeloma and displays preferential cytotoxicity for CD45+ myeloma cells. Am J Hematol. 2010;85(9):675–686.
[40] Kannaiyan R, Hay HS, Rajendran P, et al. Celastrol inhibits proliferation and induces chemosensitization through down-regulation of NF-kappaB and STAT3 regulated gene products in multiple myeloma cells. Br J Pharmacol. 2011;164(5):1506–1521.
[41] Takeda T, Tsubaki M, Tomonari Y, et al. Bavachin induces the apoptosis of multiple myeloma cell lines by inhibiting the activation of nuclear factor kappa B and signal transducer and activator of transcription 3. Biomed Pharmacother. 2018;100:486–494.
[42] Hu L, Wu H, Li B, et al. Dihydrocelastrol inhibits multiple myeloma cell proliferation and promotes apoptosis through ERK1/2 and IL-6/STAT3 pathways in vitro and in vivo. Acta Biochim Biophys Sin (Shanghai). 2017;49(5):420–427.
[43] Garcia JF, Camacho FI, Morente M, et al. Hodgkin and Reed-Sternberg cells harbor alterations in the major tumor suppressor pathways and cell-cycle checkpoints: analyses using tissue microarrays. Blood. 2003; 101(2):681–689.
[44] Mackenzie GG, Queisser N, Wolfson ML, et al. Curcumin induces cell-arrest and apoptosis in association with the inhibition of constitutively active NF-kappaB and STAT3 pathways in Hodgkin's lymphoma cells. Int J Cancer. 2008;123(1):56–65.
[45] Zhang Q, Yang Z, Jia Z, et al. ISL-1 is overexpressed in non-Hodgkin lymphoma and promotes lymphoma cell proliferation by forming a p-STAT3/p-c-Jun/ISL-1 complex. Mol Cancer. 2014;13(1):181.
[46] Zhao X, Zhang Z, Moreira D, et al. B cell lymphoma immunotherapy using TLR9-targeted oligonucleotide STAT3 inhibitors. Mol Ther. 2018;26(3):695–707.
[47] Mitchell TJ, John S. Signal transducer and activator of transcription (STAT) signalling and T-cell lymphomas. Immunology. 2005;114(3):301–312.
[48] Balkwill F, Mantovani A. Inflammation and cancer: back to Virchow? Lancet. 2001;357(9255):539–545.

[49] Hanahan D, Weinberg RA. Hallmarks of cancer: the next generation. Cell. 2011;144(5):646–674.
[50] Ribatti D. Mast cells and macrophages exert beneficial and detrimental effects on tumor progression and angiogenesis. Immunol Lett. 2013;152(2):83–88.
[51] Iriki T, Ohnishi K, Fujiwara Y, et al. The cell-cell interaction between tumor-associated macrophages and small cell lung cancer cells is involved in tumor progression via STAT3 activation. Lung Cancer. 2017;106: 22–32.
[52] Zhang X, Zeng Y, Qu Q, et al. PD-L1 induced by IFN-gamma from tumor-associated macrophages via the JAK/STAT3 and PI3K/AKT signaling pathways promoted progression of lung cancer. Int J Clin Oncol. 2017;22(6):1026–1033.
[53] Tamma R, Ruggieri S, Annese T, et al. Bcl6/p53 expression, macrophages/mast cells infiltration and microvascular density in invasive breast carcinoma. Oncotarget. 2018;9(32):22727–22740.
[54] Harris JA, Jain S, Ren Q, et al. CD163 versus CD68 in tumor associated macrophages of classical Hodgkin lymphoma. Diagn Pathol. 2012;7(1):12.
[55] Jeong J, Oh EJ, Yang WI, et al. Implications of infiltrating immune cells within bone marrow of patients with diffuse large B-cell lymphoma. Hum Pathol. 2017;64:222–231.
[56] Wang J, Gao K, Lei W, et al. Lymphocyte-to-monocyte ratio is associated with prognosis of diffuse large B-cell lymphoma: correlation with CD163 positive M2 type tumor-associated macrophages, not PD-1 positive tumor-infiltrating lymphocytes. Oncotarget. 2017; 8:5414–5425.
[57] Guo Q, Jin Z, Yuan Y, et al. New mechanisms of tumor-associated macrophages on promoting tumor progression: recent research advances and potential targets for tumor immunotherapy. J Immunol Res. 2016;2016:1.
[58] Kridel R, Steidl C, Gascoyne RD. Tumor-associated macrophages in diffuse large B-cell lymphoma. Haematologica. 2015;100(2):143–145.
[59] Chen Z, Deng X, Ye Y, et al. Novel risk stratification of de novo diffuse large B cell lymphoma based on tumour-infiltrating T lymphocytes evaluated by flow cytometry. Ann Hematol. 2019;98(2):391–399.
[60] Xu Y, Kroft SH, McKenna RW, et al. Prognostic significance of tumour-infiltrating T lymphocytes and T-cell subsets in de novo diffuse large B-cell lymphoma: a multiparameter flow cytometry study. Br J Haematol. 2001;112(4):945–949.